

Soft Storage for Hydrogen

Microporous materials based on metal-organic framework compounds offer the possibility of systematic changes in pore sizes. One family of compounds based on octahedral Zn-O-C clusters and aromatic linking groups has been shown to possess a high capacity for methane sorption under ambient conditions. **Rosi et al.** (p. 1127; see the Perspective by **Ward**) now report that one of these materials, MOF-5, also has a high capacity for hydrogen uptake. Inelastic neutron scattering spectroscopy of the rotational motion of hydrogen at 10 kelvin reveals two sharper peaks at 10.3 and 12.3 millielectron volts that correspond to binding sites to zinc and to the aromatic linker groups, respectively. At liquid nitrogen temperatures, the material adsorbs 4.5 weight percent (wt %) hydrogen, and an MOF-5 derivative adsorbs 2 wt % hydrogen at room temperature and 20 bars of pressure. The tunability of this materials system may allow it to reach the engineering goal of 6.5 wt % storage desired for automotive applications.

Magnetism of Nanoclusters

Magnetic devices usually exploit the presence of “easy” and “hard” axes of orientation of magnetization created by the interaction of the electrons with the crystal symmetry of the recording material. How does this anisotropy in magnetization change as the bit sizes are shrunk to the nanoscale? **Gambardella et al.** (p. 1130) have looked at the problem from the opposite end. They examined the magnetic anisotropy of single cobalt atoms and how it changes as nanoparticles containing a few tens of atoms are deposited on a platinum substrate. Single atoms possess a large magnetic anisotropy that appears to arise through the reduced symmetry or coordination of the orbital electrons of the magnetic adatoms. The authors suggest that such an effect could be used improve magnetic properties of nanoparticles that tend to show a reduced magnetic anisotropy as they get bigger.

Mussel Breach

Strong oceanic upwelling off the California coast results in few alternative prey for the predatory whelk, *Nucella canaliculata*, and its feeding concentrates on the drilling of mussels. Weaker upwelling off the Oregon and Washington coasts results in high barnacle recruitment, many alternative prey, and whelks less able to drill mussels. In laboratory-rearing experiments, **Sanford et al.** (p. 1135) show persistence of this behavioral difference as well as genetic distinctions among the whelk populations.

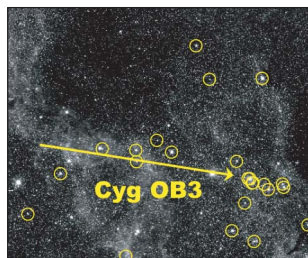
Carbon Black Box Below Ground

The below-ground compartment of terrestrial ecosystems remains poorly studied because of its physical characteristics and the micro-

Hole in the Dark

Black holes may form after a supernova explosion triggers a collapse of the core of a massive star to a neutron star. The neutron star then re-accretes some of the ejected

1119



material and gains enough mass to convert into a black hole. The supernova will also give the system a “kick” that sends it away from its birthplace at a relatively high velocity. **Mirabel and Rodrigues** (p. 1119) tested this model for the 10-solar-mass candidate black hole in Cygnus X-1. Based on a kinematic analysis of the position and space velocity of Cygnus X-1 relative to its inferred birthplace, the system ejected only a small amount of mass, much smaller than the mass ejected in a supernova explosion. The Cygnus X-1 black hole formed in the “dark” and was not triggered by a supernova explosion. ✕

scopic size of the majority of the biota. Thus, the life cycles of many soil organisms are not known, even those of important root symbionts such as mycorrhizal fungi. **Staddon et al.** (p. 1138) used ¹⁴C feeding and accelerator mass spectrometry to estimate the turnover rates of mycorrhizal mycelium in the soil. Mycorrhizal fungi use up to 20% of plant photosynthesis products; this rate of carbon turnover is significant even within the context of the global carbon balance.

Unbiased Increases in Diversity

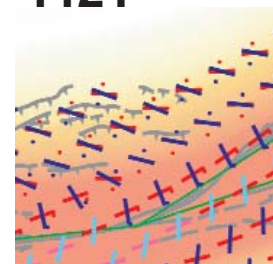
The diversity (number of genera and species) of many animals and plants seems to increase dramatically through the Tertiary (the past 65 million years), but is this simply

a bias introduced by more complete sampling? **Jablonski et al.** (p. 1133; see the news story by **Kerr**) have tested this effect by examining the fossil record of bivalves in the Pliocene and Pleistocene, the times closest to the Recent record. They find that the “Pull of the Recent” is but a slight tug, and that the bias is minimal for this well-studied group. They conclude that the observed five-fold increase in bivalve genera, and similar increases in many other genera, is real.

Giving and Taking the Slip

The simple view of plate tectonics, is that one plate moves past another, but the process is often much more complex and involves partitioning of slip motion on different faults (see the Perspective by **Jones**). The Denali fault earthquake on 3 November 2002 had a large moment magnitude of 7.9 and ruptured about 327 kilometers of the surface in Alaska. **Eberhart-Phillips et al.** (p. 1113; see the cover) found that most of the rupture was directed in a right-lateral strike-slip motion along the Denali and Totschunda faults with a maximum horizontal offset of 8.8 meters. The velocity and directivity of the rupture produced strong surface deformation and enhanced seismicity in volcanic regions as far as 4000 kilometers from the epicenter. The partitioning of slip into three subevents and strong directivity effects provide rare and important observations about large earthquakes. Oblique compression along major plate boundaries is often partitioned into slip on different types of faults. **Bowman et al.** (p. 1121) suggest that oblique slip on a localized shear zone in an elasto-plastic lower crust can cause slip partitioning in the brittle upper crust as the fracture propagates upward. Their relatively simple model can explain the relatively complex slip partitioning observed in southern California and northeastern Tibet.

1121



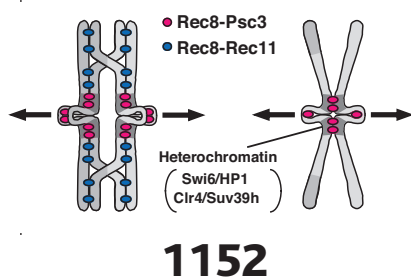
CONTINUED ON PAGE 1051

Increasing Insulin Resistance with Age

Type 2 diabetes is especially prevalent in the elderly population. **Petersen *et al.*** (p. 1140) used nuclear magnetic resonance (NMR) spectroscopy to measure *in vivo* metabolic function in healthy elderly volunteers. Compared with young adults, the elderly subjects were markedly insulin-resistant. This condition was accompanied by an increase in liver and muscle fat and, remarkably, a 40% decline in mitochondrial oxidative and phosphorylation activity in skeletal muscle. Thus, age-associated mitochondrial dysfunction may contribute to the onset of diabetes in the elderly.

Making and Breaking an Antiviral Response

Viral infection activates type I interferon genes. This process requires the cooperative activation of several transcription factors, including interferon regulatory factor (IRF)-3 and IRF-7 (see the Perspective by **Williams and Sen**). Signals such as double-stranded RNA lead to the phosphorylation of IRF-3 and IRF-7 by a yet-uncharacterized virus-activated kinase (VAK). **Sharma *et al.*** (p. 1148) now show that the component of VAK responsible for IRF-3 and IRF-7 phosphorylation is IKK ϵ /TBK-1, an IKK-related kinase. **Foy *et al.*** (p. 1145) observed that the hepatitis C virus (HCV) serine protease (NS3/4A) blocks IRF-3 phosphorylation. Thus, HCV has evolved a mechanism of obstructing the cellular interferon response, potentially through the proteolytic cleavage of IKK ϵ /TBK-1. **X**



Chromosomes On the Move

Meiosis, the production of haploid egg and sperm cells with only half the DNA content of the diploid parent cells, requires a complex series of movements that are orchestrated in part by cohesins, proteins that hold homologous chromosomes together. **Kitajima *et al.*** (p. 1152) show that distinct cohesin complexes are required for distinct steps in meiosis. A Rec8-Rec11 complex plays an essential role in chromosome arm cohesion during the first meiotic

division by ensuring effective recombination of the maternal and paternal genomes. A Rec8-Psc3 complex supports centromeric cohesion during both the first and second meiotic divisions and establishes monopolar attachment to the spindle during the first division and proper sister chromatid alignment in the second.

Rethinking Tumor Radiotherapy

Nearly half of all cancer patients are treated with radiation therapy. The magnitude of the tumor response to ionizing radiation is thought to be determined primarily by the death rate of tumor stem cells. **Garcia-Barros *et al.*** (p. 1155) show instead that endothelial cells within the tumor play a major role in determining radiation sensitivity. Murine tumors became radiation resistant when their endothelial cells were made resistant to ionizing radiation by genetic inactivation of acid sphingomyelinase, an enzyme required for endothelial cell apoptosis. These results suggest that optimal targeting of tumors by radiotherapy may have to take into account endothelial responses.

Look, Ma, No Factors!

The ribosome moves along the messenger RNA (mRNA) to read out the three-nucleotide codons for protein synthesis. Normally, this movement is promoted by a conformational change in elongation factor G (EF-G); binding of EF-G to the ribosome liberates energy by stimulating the hydrolysis of the bound guanosine triphosphate to drive the conformational change. **Fredrick and Noller** (p. 1159) show that the peptidyl-transferase inhibitor sparsomycin can, unexpectedly, induce a factor-independent translocation of the ribosome along the mRNA. Thus, the change from substrate to product in the peptidyl-transfer center in the large ribosomal subunit supplies enough information and energy to move the mRNA through the decoding center in the small ribosomal subunit, some 50 angstroms distant.